Pharmaceutical Research, Volume 23, No. 2, February 2006 (© 2006)
DOI: 10.1007/s11095-005-9258-5

Research Paper

Transport Kinetics of Iron Chelators and Their Chelates in Caco-2 Cells

Xi-Ping Huang,[1] M. Spino,[1,2] and J. J. Thiessen[1,3]

Received June 14, 2005; accepted October 25, 2005

Purpose. Caco-2 monolayers were used to contrast the bidirectional transport of iron chelators and their chelates and to estimate fundamental kinetics associated with their intestinal absorption.
Methods. Bidirectional transport was studied at 37°C and pH 7.4 using 500-μM concentrations. Monolayer integrity was tested via transepithelial electrical resistance and sodium fluorescein permeability. Apical and basolateral analysis provided mass balance evidence. Apparent permeability coefficient (P_{app}) served to rank and compare molecules and estimate *in vivo* bioavailability. Model-dependent rate constants defined cellular influx and efflux.
Results. 1) P_{app} ranked in decreasing order for chelators from directional transport studies were CP363 > deferiprone> ICL670 > CP502 > deferoxamine (DFO). 2) $Fe(CP502)_3$, $Fe(ICL670)_2$, and FeDFO were not measurable in receiving chambers, whereas $Fe(deferiprone)_3$ and $Fe(CP363)_3$ were detected in both directions. 3) CP363 was transported significantly faster from the basolateral to the apical direction than the converse. 4) Mass balance of donor and receiver chambers gave approximately 100% recovery in all cases. 5) Kinetic analysis supports the view that the Caco-2 chelator efflux constants are generally greater than their influx constants.
Conclusions. Caco-2 cells are useful in screening iron chelators and chelates and estimating bioavailabilities. Structure and distribution coefficients partially predict passive transport through Caco-2 monolayers.

KEY WORD: Caco-2 cells; iron chelate; iron chelator; iron overload.

INTRODUCTION

Millions of people suffer from iron overload that, if untreated, causes death. Iron chelation therapy has significantly increased the life span of patients who suffer from iron-overload diseases such as β-thalassemia major. Deferoxamine (DFO) and deferiprone (CP20) are the only two iron chelators currently in clinical use. DFO has been extensively used in clinical practice since 1970. Unfortunately, it is orally inactive and has a high plasma clearance with a half-life of 5–10 min. Therefore, long subcutaneous infusions (8–12 h/day, five to seven times per week) are required to maintain an adequate chelator concentration in the blood. The expense and complexity of the treatment limit its use, particularly in some underdeveloped countries. Even in those countries where it is used, the difficulty of the regimen substantially lessens the patient's quality of life (1–3). Clinical trials have shown that deferiprone promotes urinary iron excretion comparable to DFO. Although deferiprone is orally available, the chelating efficacy is limited by competing rapid biotransformation with up to 85% metabolized to a nonchelating 3-*o*-glucuronide conjugate. To keep patients in negative iron balance, a dose as high as 75–100 mg/kg of body weight per day is needed. Furthermore, deferiprone-related adverse effects, such as arthralgia, severe neutropenia, or agranulocytosis, have also been reported (2–4).

The clinical limitations of DFO and deferiprone have caused a concerted search for more effective oral iron chelators. Such candidates would be readily absorbed. Hepatic first-pass effects should at most be intermediate so that adequate chelation might also potentially occur outside liver in nonhepatic regions. The resultant chelates should be efficiently eliminated from the body without redistribution. In addition, the chelates formed in the gastrointestinal lumen after oral administration should not enter the body. Otherwise, dietary iron (e.g., 5–6 mg per 1000 kcal and a total daily iron intake of 12–18 mg in a typical Western diet) could potentially be brought into the body via orally ingested chelators.

Rapid preclinical screening of both chelators and their iron chelates could assist in identifying potential new orally administered candidates. Caco-2 cells are an epithelial cell line originally derived from a human colorectal adenocarcinoma. When cultured on the permeable membrane filter, these cells spontaneously differentiate into enterocytes and form polarized monolayers, possessing distinct apical, basolateral membranes and tighter junctions between adjacent cells. The apical side has a well-developed brush border with transport systems, enzymes, ion channels that mimic the characteristics of the small intestine. Because of these properties, the Caco-2 cell model has become an important

[1] Leslie Dan Faculty of Pharmacy, University of Toronto, 19 Russell St., Toronto, Ontario, Canada, M5S 2S2.
[2] ApoPharma, Toronto, Ontario, Canada.
[3] To whom correspondence should be addressed. (e-mail: jj.thiessen@utoronto.ca)

tool in the *in vitro* assessment or prediction of oral permeability in humans. Importantly for our studies, Caco-2 cells also express the key genes and proteins involved in iron transport and storage, including the divalent metal transporter (DMT1), transferrin receptor, ferritin, iron-regulated transporter (IREG1), plasma ferrireductase activity, Dcytb, and hephaestin (5–10). This is important for evaluating the potential intestinal transport of iron chelates.

The purpose of this study was to establish rapid preclinical screening methodologies for both chelators and their iron chelates. Given the intended oral administration of new molecules, we chose to use Caco-2 as a model system to investigate the intestinal transport of several iron chelators and chelates representing different classes of molecular structure. Fundamentally, our goal was to contrast the bidirectional transport of the selected molecules and to estimate basic kinetic properties associated with their intestinal absorption. We report herein our observations with chelators that are either currently in preclinical development (CP363 and CP502), in phase III clinical trials (ICL670), or in clinical use (DFO and deferiprone) (11,12). The molecular structures of these compounds are shown in Fig. 1.

MATERIALS AND METHODS

Materials

Caco-2 cells (HTB-37, passage 18) were obtained from the American Type Culture Collection (Rockville, MD, USA). Dulbecco's modified Eagle's high glucose medium (DMEM), fetal bovine serum (FBS), nonessential amino acids, trypsin–ethylenediaminetetraacetic acid (EDTA), and penicillin/streptomycin were obtained from Invitrogen (Toronto, ON, Canada). Tissue culture plastics and polycarbonate Transwell® filters with a pore size of 0.4- and 12-mm diameter were obtained from Corning-Costar (Corning, NY, USA).

Other than as indicated, all chemicals and reagents were obtained from Sigma (Oakville, ON, Canada). CP363 and FeDFO were gifts from Dr. R. Hider (Department of Pharmacy, King's College of London, UK); deferiprone and Fe(deferiprone)$_3$, CP502, Fe(CP502)$_3$, ICL670, Fe(ICL670)$_2$, and Fe(CP363)$_3$ were provided from Apotex Inc. (Toronto, ON, Canada). Sodium fluorescein was obtained from Molecular Probes, Inc. (Eugene, OR, USA).

Cell Culture

Caco-2 cells were maintained in DMEM containing 2 mM L-glutamine, supplemented with 10% FBS, 0.1 mM nonessential amino acid, 100 U/ml penicillin, and 100 μg/ml streptomycin. The cells were cultured at 37°C in a humidified atmosphere with 5% CO_2. Cells were passaged at 80–90% confluence using 0.05% trypsin–EDTA, and medium was changed every other day during T-flask culture. To prepare monolayers for transport studies, Caco-2 cells (passages 20–40) were cultured on polycarbonate Transwell inserts (above) in 12-well plates at a density of 62,000 cells/cm^2. Cells were fed 24 h postseeding and then every other day before use.

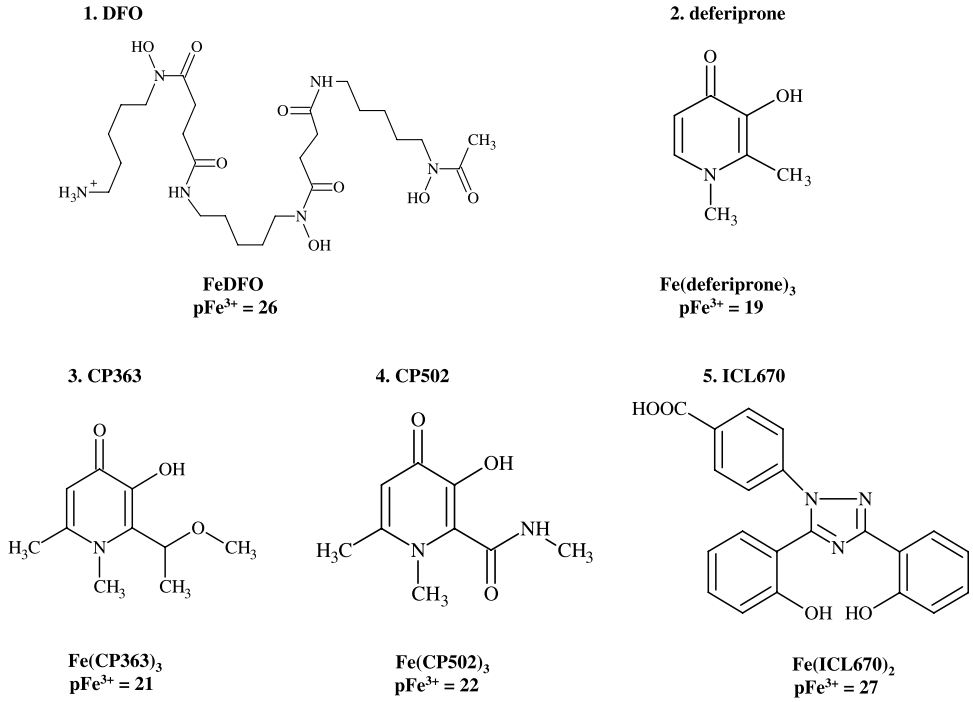

Fig. 1. Molecular structures of iron chelators. Deferoxamine (DFO) (1) is a hexadentate hydroxamate iron chelator naturally secreted from the microorganism *Streptomyces pilosus*. It forms a 1:1 iron complex. Deferiprone (2), CP363 (3), and CP502 (4) belong to the family of bidentate 3-hydroxypyridin-4-one ligands and form a 1:3 iron complex. ICL670 is a tridentate ligand, and it forms a 1:2 iron complex. pFe^{3+} is defined as the negative logarithm of the free Fe^{3+} concentration. It is determined at iron and chelator concentrations of 1 and 10 μM, respectively, at pH 7.4. The iron complex form and its pFe^{3+} values are listed under its chelator molecular structure.

Transport Studies

Transport studies were conducted on the Caco-2 monolayers after 21–23 days in culture. Other than ICL670, all compounds were prepared in the Krebs–Ringer buffer (KRB) containing 10 mM HEPES (pH 7.4), 25 mM glucose, 1.1 mM $MgCl_2$, 1.25 mM $CaCl_2$, 114 mM NaCl, 5 mM KCl, 20 mM $NaHCO_3$, 1.65 mM Na_2HPO_4, and 0.3 mM NaH_2PO_4. ICL670 was first dissolved in dimethyl sulfoxide (DMSO) then diluted in KRB to give a final maximum DMSO concentration of 1% v/v. For studies of the corresponding iron complex, an equal molar concentration of its chelator was included to limit the possibility of iron dissociation from its complex. Other than CP363, all chelators and chelates were tested at a concentration of 500 μM. CP363 was tested using concentrations from 100 μM to 5 mM.

On the day of the experiment, cell monolayers were first washed three times with prewarmed KRB and then incubated in the buffer with 0.5 ml added to the apical side and 1.5 ml to the basolateral side for 2–3 h at 37°C until the transepithelial electrical resistance (TEER) value reached its steady state. TEER values were measured using EVOM® epithelial voltohmmeter (Millipore, Billerica, MA, USA). The preincubation buffer was then aspirated and replaced with new KRB containing the test compound added either to the apical (apical to basolateral transport, A-to-B) or the basolateral (basolateral to apical transport, B-to-A) chamber.

The experiments were performed at 37°C with constant mixing on an orbital shaker at a speed of 50 rpm. Samples were collected under two experimental conditions, designated as sink and nonsink conditions. Under sink conditions, samples from the receiver chamber were collected and replaced with prewarmed KRB at specific time points (30, 60, 90,120, or 180 min). The remaining medium in the donor chamber was also collected at the end of experiment. For nonsink conditions, samples from both donor and receiver chambers were collected after each incubation period. TEER values were measured before and at set times during the course of the experiment. Sodium fluorescein (10 μg/ml in KRB) was added to the donor chamber at the end of experiment, and the leakage of sodium fluorescein was detected from the receiving chamber after 60-min incubation.

A decrease in TEER and leakage of fluorescein marker is indicative of cellular disruption or membrane damage during the experiment. No membrane damage was observed in the studies.

Mass Balance Study

Mass balance was determined by analyzing samples collected from both the donor and receiver chambers at the end of the experiment. This approach permitted potential cellular accumulation, metabolism, or adsorption of probes to the plasticwares from clouding the observations. Recovery was calculated as the total mass transferred into the receiver chamber along with the mass remaining in the donor chamber *vs.* the initial mass added to the donor.

Distribution Coefficient

Octanol/buffer distribution coefficients (log $D_{7.4}$) were determined spectrophotometrically as described by Streater *et al.* (13) for both chelators and their chelates. Briefly, chelators or chelates were prepared at a concentration of between 0.1 and 0.5 mM in KRB (pH 7.4) and equilibrated with a volume of octanol by shaking overnight at 25°C. The concentration was chosen to give a UV absorbance of 0.8–1.3 before octanol extraction, whereas the volume of octanol was chosen to give a decrease of between 30 and 70% in the absorbance of the buffer layer after equilibration. The wavelength used for each compound was identical to that used in high-performance liquid chromatographic (HPLC) analysis in Table I. The log $D_{7.4}$ of chelates was detected in the presence of an equal mole of their chelators.

Analytical Methods

The HPLC system was a Hewlett-Packard 1050 Series (Waldbronm, Germany) and consisted of an HP 1050 Series pump, an HP 1050 Series autosampler (1–100 μl), and an HP 1050 Series UV–visible detector (200–500 nm) controlled by a computer employing the HP ChemStation software. An Xterra MS 18 (C-18) column from Waters (5 μm; 4.6 × 250 mm; Milford, MA, USA) was used for the determination of ICL670,

Table I. HPLC Conditions for the Analytics

	Column	Mobile phase		Detection (nm)	Flow rate (ml/min)
		Buffer	ACN (%)		
Deferiprone	Hamilton, C-18	95% H_2O TFA, pH 1.5	5	280	0.8
CP363	Hamilton, C-18	85% H_2O TFA, pH 1.5	15	280	0.8
CP502	Hamilton, C-18	88% H_2O TFA, pH 1.5	12	280	0.8
ICL670	Xterra, C-18	40% 2 mM EDTA in 10 mM MOP, pH 7.4	15	280	0.8
DFO	Xterra, C-18	85% 10 mM Tris–HCl, pH 7.4	15	214	0.8
$Fe(deferiprone)_3$	Xterra, C-18	88% 0.5 mM deferiprone in 10 mM Tris–HCl, pH 7.4	12	430	0.8
$Fe(CP363)_3$	Xterra, C-18	65% 0.5 mM CP363 in 10 mM Tris–HCl, pH 7.4	35	430	0.8
$Fe(CP502)_3$	Xterra, C-18	88% 0.5 mM CP502 in 10 mM Tris–HCl, pH 7.4	12	430	0.8
$Fe(ICL670)_2$	Xterra, C-18	88% 0.1 mM ICL670 in 10 mM Tris–HCl, pH 7.4	12	430	0.8
FeDFO	Xterra, C-18	88% 0.1 mM DFO in 10 mM Tris–HCl, pH 7.4	12	430	0.8

HPLC: High-performance liquid chromatography; ACN: acetonitrile; TFA: trifluoroacetic acid; EDTA: ethylenediaminetetraacetic acid; MOP: 3-(*N*-morpholino)-propanesulfonic acid.

DFO, and all iron chelates; a Hamilton PRP-1 polymer column (C-18) (5 μm; 4.6 × 200 mm; Reno, NV, USA) was used for deferiprone, CP363, and CP502. The HPLC conditions are listed in Table I. The sample injection volume was 100 μl. The compounds were identified according to peak retention times and UV spectra. The concentrations of compounds were determined by UV detection (214 nm for DFO, 280 nm for all other chelators, and 430 nm for the chelates) with reference to linear ($r^2 > 0.99$) calibration curves (data not shown). Calibration standards for each compound were prepared in the transport buffer and run on each day of analysis. The limit of quantitation (LOQ) for deferiprone, CP363, CP502, and ICL670 was 0.5 μM, whereas 1 μM was the LOQ for DFO and all iron chelates. All the measurements were performed at ambient temperature. Samples were analyzed either after collection or stored at −20°C until analyzed in less than a 1-week period. Stability of molecules was maintained during any brief storage.

Sodium fluorescein was determined via a 96-well plate reader from Molecular Devices (Sunnyvale, CA, USA) at an excitation wavelength of 488 nm and emission wavelength of 530 nm.

Calculations

Apparent Permeability Coefficient

Apparent permeability (P_{app}, cm/s) was calculated using the following equations:

$$\textit{Sink conditions}: P_{app} = (dQ/dt)/(A \cdot C_o) \quad (1)$$

$$\textit{Non-sink conditions}: \quad (2)$$

$$P_{app} = V_R \cdot (dC_R/dt)/[A \cdot (C_D - C_R)]$$

where dQ/dt (nmol s^{-1}) is the flux rate of mass transport across the monolayers, A is the surface area of the insert membrane (1.13 cm^2), and C_o is the initial concentration (μM) of the compound in the donor chamber. C_D and C_R are the drug concentrations at the donor side and receiver side, respectively. V_R is the volume of the receiver chamber. The flux rates were determined by plotting the cumulative amount of test compound permeated as a function of time and determining the slope via linear regression.

Kinetic Model and Parameter Estimation

A three-compartment model with first-order transfer constants was used to describe chelators across Caco-2 monolayers. A schematic description of the model is shown in Fig. 2.

The following equations define the drug concentrations at any given time (t) in the apical, cellular, and basolateral compartments [$C_a(t)$], [$C_c(t)$], and [$C_b(t)$], respectively.

For A-to-B directional transport:

$$C_a(t) = (-k_{12}C_aV_a + k_{21}C_cV_c)/V_a \quad (3)$$

$$C_b(t) = (-ik_{32}C_bV_b + k_{23}C_cV_c)/V_b \quad (4)$$

$$C_c(t) = (k_{12}C_aV_a - (k_{21} + k_{23})C_cV_c)/V_c \quad (5)$$

For B-to-A directional transport:

$$C_a(t)' = (-ik_{12}C_aV_a + k_{21}C_cV_c)/V_a \quad (6)$$

$$C_b(t)' = (-k_{32}C_bV_b + k_{23}C_cV_c)/V_b \quad (7)$$

$$C_c(t)' = (k_{32}C_bV_b - (k_{21} + k_{23})C_cV_c)/V_c \quad (8)$$

where k_{12} and k_{32} are influx rate constants from the apical and the basolateral to the cellular compartment, respectively, whereas k_{21} and k_{23} present efflux rate constants for chelators' flux out from cellular compartment to the apical and basolateral chambers, respectively. ik_{32} and ik_{12} are the corresponding back-diffusion rate constants for A-to-B and B-to-A transports. However, it was assumed that under experimental sink conditions, there is no back-diffusion once molecules enter the receiving chamber, where ik_{32} and ik_{12} are equal to 0. V is the volume of the compartment with V_a of 0.5 cm^3 for the apical, V_b of 1.5 cm^3 for the basolateral, and V_c of 0.028 cm^3 for the cellular compartment of a Caco-2 monolayer with an area of 1.13 cm^2. The cellular volume of 0.028 cm^3 was calculated on the geometrical dimensions of the Transwell insert with a radius of 6 mm and a height of the

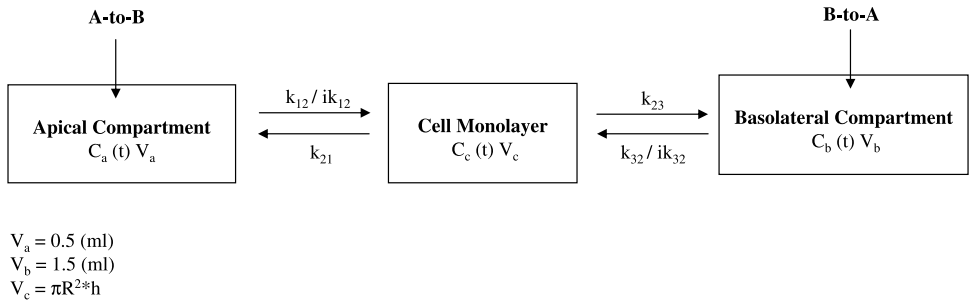

Fig. 2. Schematic presentation of the Caco-2 model containing an apical compartment, a cell monolayer compartment, and a basolateral compartment. $C(t)$ is the drug concentration at any given time. C_a and C_b represent the concentrations in the apical and the basolateral chambers, respectively, whereas C_c is representative of the concentrations in the cellular compartment. V is the volume (ml) in the apical chamber (V_a), basolateral chamber (V_b), and the cell monolayer (V_c). V_c was calculated from the equation of $\pi R^2 h$, where π is 3.14, R is the radius of the Transwell insert (6 mm), and h is the height of the monolayers (25 μM) estimated from the image of light microscopy of Caco-2 monolayers by Liang *et al.* (28).

monolayers of 25 μm (28). Nonlinear least-squares regression, using Scientist (MicroMath, St. Louis, MO, USA), was used to fit the concentration-time data from both directional transport studies simultaneously to estimate k_{12}, k_{32}, k_{21}, and k_{23}.

Distribution Coefficient

The distribution coefficient was defined as the ratio of the concentration of chelators or chelates in octanol to that in KRB. It was calculated from:

$$\log D = \log [(\mathrm{Abs}_1 - \mathrm{Abs}_2)V_B/\mathrm{Abs}_2 V_o] \quad (9)$$

where Abs_1 is the absorbance of test compound in KRB before octanol extraction, whereas Abs_2 is representative of the absorbance after octanol extraction. V_B is the volume of KRB, and V_o is the volume of octanol.

Statistical Analysis

The results herein are expressed as the mean ± SD. Statistical significance was determined via a nonpaired Student's t test (between two groups) or by analysis of variance and Duncan's multiple range test (more than two groups). Values of p exceeding 0.05 were considered insignificant.

RESULTS

HPLC Methodology

Calibration curves containing chelators or chelates were constructed over the analytical range of 5–500 μM by using the analytes in transport buffer at pH 7.4. Linear regression defined the relationship between peak areas and on-column injected amounts (in nanomoles). For all compounds, correlation coefficients of 0.999 were obtained for the on-column ranges (0.125–50 nmol). Intraday accuracy and precision were determined using two different concentrations, with five to six replications per concentration. This was repeated on three separate occasions to identify the interday accuracy and precision. For all chelators and their chelates, the intra- and interday coefficients of variation were less than 5%. Using a signal-to-noise ratio of 10, the LOQ for deferiprone, CP363, CP502, and ICL670 in the solution was 0.5 μM (0.05 nmol injected), whereas 1 μM (0.1 nmol injected) was the LOQ for DFO and all chelates.

Integrity of Caco-2 Monolayers

The tight junctions (paracellular permeability) of cell monolayers were evaluated by measuring TEER values and by studying the permeability of sodium fluorescein, a hydrophilic marker, across the monolayers. The measured TEER values were 344 ± 96 Ω cm^2 (mean ± SD; n = 193). The permeability of sodium fluorescein (10 μg/ml) from both directions was tested on the monolayers with a TEER value of 212 ± 19. Less than 0.01% of sodium fluorescein was recovered from the receiver chambers for transport in both directions.

Transport of Chelators and their Chelates across Caco-2 Monolayers

The P_{app} values from bidirectional transport of chelators and their chelates are summarized in Fig. 3. No significant decrease in TEER values was observed for all chelators and

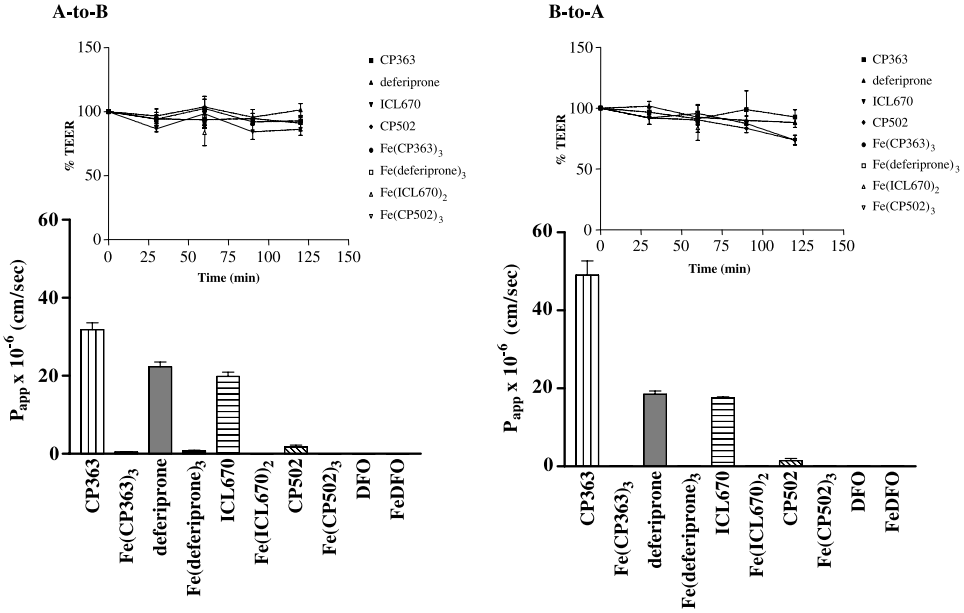

Fig. 3. Bidirectional transport of iron chelators and their chelates. Left panel shows the apparent permeability coefficient (P_{app}) values from A-to-B transport of chelators and their chelates. Right panel represents the results from B-to-A transport of these compounds. The inserts from both panels show % TEER changes after incubation with the test compounds. Data are presented as mean ± SD (n = 4–6 monolayers).

their chelates at a concentration of 500 μM during and at the end of the incubation period from the apical to the basolateral direction as well as from the basolateral to the apical direction (Fig. 3 inserts). No fluorescein leakage (less than 0.01%) was detected from the receiving chambers for both directional transport studies at the end of the study for all cases. This indicated that the monolayers remained intact throughout the incubation period, and the chelators and their chelates had no toxic effect on Caco-2 monolayers at the concentrations tested.

Mass balance study showed 85–110% recovery for all compounds. No metabolites or other degradation products were observed in the HPLC analysis.

Bidirectional Transport of Deferiprone, CP363, CP502, and ICL670

Bidirectional transport of this group of chelators was performed under experimental sink conditions to avoid potential bias by back-diffusion of a significant amount of drug from the receiving chamber. The permeability coefficients from both directions were measured in the absence of a pH gradient (pH 7.4 at both the apical and the basolateral chambers) at a concentration of 500 μM.

The P_{app} values calculated from the slope of the curves (Fig. 4) are summarized in Table II. No significant differences in the P_{app} values from A-to-B *vs.* B-to-A transport of CP502, deferiprone, and ICL670 were found, whereas a significant difference was observed for the transport of CP363; CP363 was transported considerably faster from B-to-A than from A-to-B.

Transport of DFO and Iron Chelates

Our initial transport studies using DFO and some of the iron chelates showed that little of these compounds were able to cross Caco-2 monolayers. Therefore, for these species, the transport study was conducted under experimental nonsink conditions without a pH gradient. After 60-min incubation, amount of drugs detected from receiving chamber was used to calculate P_{app} values. For iron chelates, to eliminate the potential dissociation of iron from its chelator, an equimolar concentration of its chelator was included in the solution.

Neither DFO, $Fe(CP502)_3$, nor $Fe(ICL670)_2$ was able to cross the Caco-2 monolayers from either direction. However, small amounts of $Fe(CP363)_3$ and $Fe(deferiprone)_3$ were recovered from the receiving chambers from transport in both directions. The calculated P_{app} values for $Fe(CP363)_3$ are $4.47 \times 10^{-7} \pm 0.59$ cm/s for A-to-B and $2.52 \times 10^{-7} \pm 0.25$ cm/s for B-to-A, whereas $7.80 \times 10^{-7} \pm 1.48$ and $1.34 \times 10^{-7} \pm 0.27$ cm/s were the calculated values for $Fe(deferiprone)_3$ from A-to-B and B-to-A transport, respectively. Mass balance showed that essentially 100% of these compounds were recovered from the sum of transported and untransported chambers (data not shown).

Transport of CP363: Concentration and pH-Dependent Studies

To evaluate further whether the asymmetric transport of CP363 is concentration dependent, bidirectional transport of CP363 was tested. The experiments were again performed

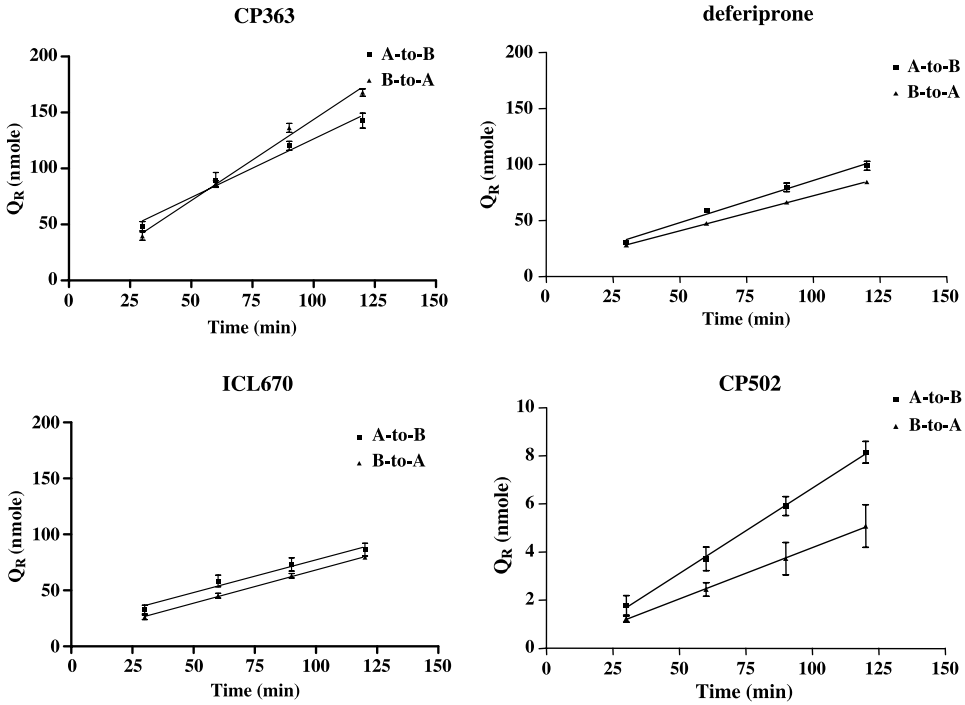

Fig. 4. Time-dependent transport studies. The experiments were conducted under sink conditions from A-to-B and B-to-A directions. Cumulative amount of the drug (Q_R, nmol) defines movement of drug into the receiving chamber. The flux rate (dQ/dt) from the slope of the curve was used to calculate P_{app}. Data are presented as mean ± SD (n = 4–6 monolayers).

Table II. Permeability Coefficients and Physicochemical Properties of Chelators and their Chelates

Compound	Permeability coefficients P_{app} ($\times 10^{-6}$ cm/s) A-to-B	B-to-A	Distribution coefficients log D (octanol/buffer pH 7.4)
Deferiprone	22.3 ± 1.2	18.5 ± 0.8	−0.8
CP363	31.8 ± 1.8	42.9 ± 4.8[a]	−0.7
CP502	1.6 ± 0.5	1.5 ± 0.5	−1.6
ICL670	16.6 ± 1.3	17.5 ± 0.3	−0.1
DFO	u.d.	u.d.	−1.7
$Fe(deferiprone)_3$	0.8 ± 0.2	0.1 ± 0.0	−2.0
$Fe(CP363)_3$	0.5 ± 0.1	0.3 ± 0.0	−1.1
$Fe(CP502)_3$	u.d.	u.d.	−2.0
$Fe(ICL670)_2$	u.d.	u.d.	−1.9
FeDFO	u.d.	u.d.	−1.8

Values are mean ± SD (n = 3–6 monolayers) or mean of two measurements without SD; A-to-B represents the measurement from the apical to the basolateral direction, whereas B-to-A is from the basolateral to the apical side.
P_{app}: permeability coefficient measured from Caco-2 monolayers; log D: distribution coefficient; u.d.: undetectable.
[a] $p < 0.05$.

under sink conditions with a non-pH gradient system. Unsaturable transport of CP363 (0.1–5 mM) was observed (Fig. 5). This suggested that the permeability of CP363 is not concentration dependent, and CP363 is passively absorbed.

Previous studies have demonstrated that the pH on the apical donor side can significantly affect transport of weak acid/base compounds because of molecule ionization (14). In addition, pH also plays an important role in the permeability of compounds utilizing proton-coupled transporters. Therefore, the pH effect on transport of CP363 was also tested. Under experimental conditions, CP363 was transported in the A-to-B direction with pH varying from 5.4 to 8.4 at the apical side and a pH of 7.4 at the basolateral side. No significant differences were observed in the P_{app} values (Fig. 6) at the tested pH conditions compared to the values obtained with a pH 7.4 in both chambers.

TEER values were not significantly altered over the tested pH range. However, the permeability of sodium fluorescein was significantly increased from less than 0.01% at pH 7.4 to 7% at pH 5.4. Because TEER values were not affected under the experimental conditions, the leakage of sodium fluorescein at pH 5.4 may be caused by transport of the unionized form of sodium fluorescein.

To test further whether experimental methods had any effect on the estimated permeabilities of iron chelators, transport was compared under sink and nonsink conditions. The permeability of CP363, CP502, and ICL670 at 500 μM was tested in the A-to-B direction under nonsink conditions at pH 7.4. Samples were collected from both donor and receiver chambers at each time point. Each value was generated from three individual Transwell inserts. The appearance and disappearance kinetics are shown in Fig. 7. A similar P_{app} was obtained under sink and nonsink conditions for CP363 and ICL670, but not for CP502.

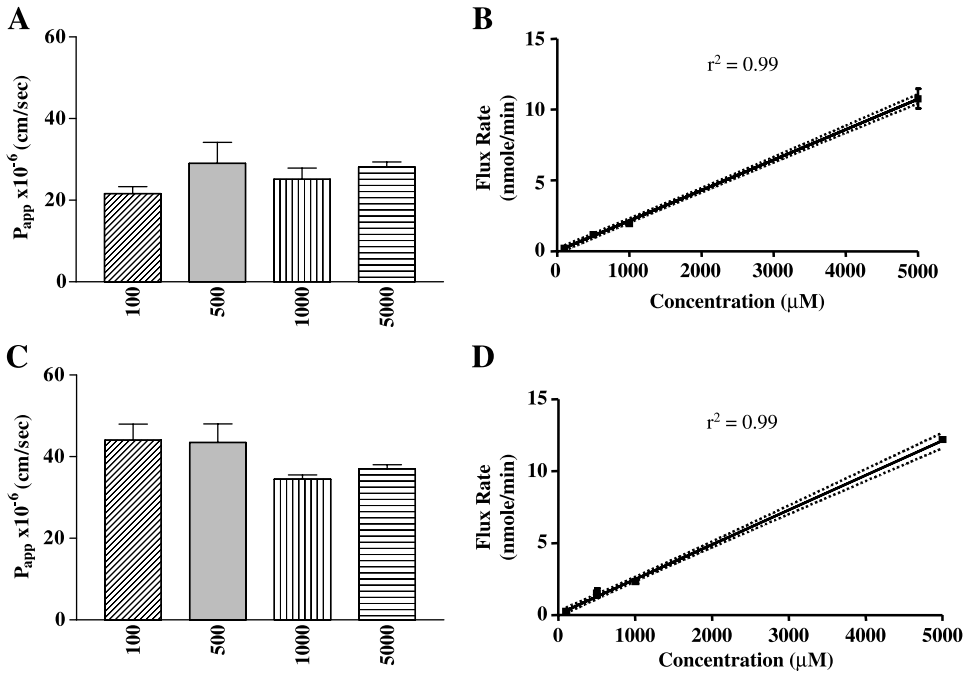

Fig. 5. The effect of concentration on A-to-B and B-to-A CP363 transport in Caco-2 monolayers. A and C: The apparent permeability coefficients obtained from A-to-B and B-to-A transport studies, respectively. A linear relationship between the A-to-B and the B-to-A flux was observed from 100 to 5000 μM (B and D, respectively). Each bar and data point represents the mean ± SD (n = 3–4 monolayers).

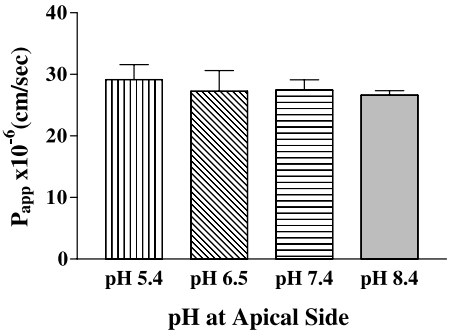

Fig. 6. The role of pH in the transport of CP363 from the apical (pH 5.4–8.4) to the basolateral (pH 7.4) direction across Caco-2 monolayers. Compared to pH 7.4, no significant differences were observed in the apparent permeability coefficient (P_{app}) at the tested pH conditions. Specific comparisons with pH 7.4 values were as follows: for pH (5.4:7.4), $p = 0.30$; for pH (6.5:7.4), $p = 0.92$; for pH (8.4:7.4), $p = 0.47$. Each bar indicates the mean ± SD (n = 3–4 monolayers).

Kinetic Parameter Estimation

Using a three-compartment model, we were able to simultaneously fit all data collected from both directional transport studies under experimental sink conditions. The rate constants influx and efflux from both the apical and the basolateral membranes are summarized in Table III. The relationships reflecting best fits are shown in Fig. 8. The kinetic analysis also supports the view that the Caco-2 efflux constants for the tested chelators are generally greater than the cellular influx constants.

Distribution Coefficient

Lipophilicity, ionization state, and molecular size are three major factors that influence the ability of a compound to freely permeate a lipid membrane (15,16). In general, a compound should possess appreciable lipid solubility ($-0.5 <$ log $D_{7.4} < 2$) to facilitate penetration of the gastrointestinal tract and achieve efficient oral absorption (13,15). To test whether oral absorption of chelators and their chelates can be also predicted by their molecular structures, we measured log D of the chelators and their chelates at pH 7.4 using octanol as organic solvent and KRB as the aqueous buffer system. The log $D_{7.4}$ values (Table II) ranked in decreasing order were as follows: ICL670 > CP363 > deferiprone > $Fe(CP363)_3$ > CP502 > DFO > FeDFO > $Fe(ICL670)_2$ > $Fe(CP502)_3$ = $Fe(deferiprone)_3$. The chelates, except FeDFO, are more hydrophilic than their chelators. $Fe(CP502)_3$, $Fe(CP363)_3$, and $Fe(deferiprone)_3$ are 2.3, 2.5, and 2.5 times more hydrophilic than CP502, CP363, and deferiprone, respectively. For ICL670, a 68-fold difference was obtained. $Fe(ICL670)_2$ is much more hydrophilic than

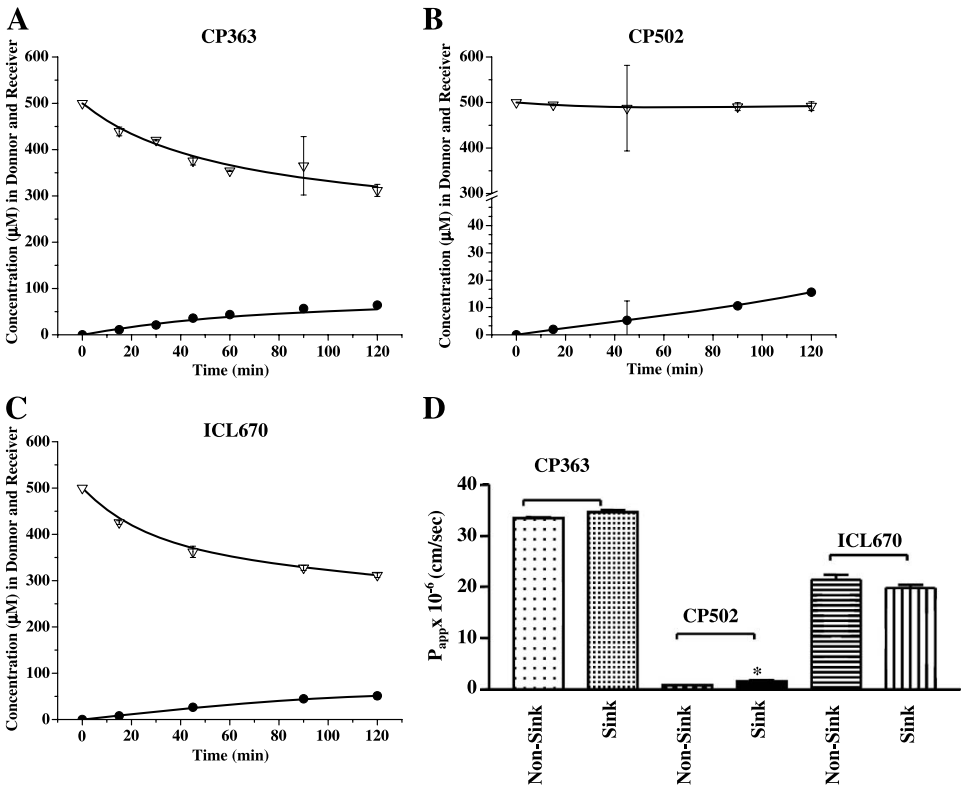

Fig. 7. The A-to-B permeability of CP363, CP502, and ICL670 at 500 μM under nonsink conditions. P_{app} values were calculated from the flux rate generated from 0 to 90 min and compared to the values obtained under sink conditions (D). A significant difference was observed for CP502 between nonsink and sink conditions ($p = 0.014$), whereas the experimental conditions had no effect on the transport of CP363 ($p = 0.44$) and ICL670 ($p = 0.23$). Data are presented as the mean ± SD (n = 3–4 monolayers for each time points). A–C: The concentration of each compound appearing and disappearing from receiver (•) and donor (▽) chambers, respectively, as a function of time.

Table III. Rate Constants Estimated from the Computer Fitting

	k_{12} (1/min)	k_{21} (1/min)	k_{23} (1/min)	k_{32} (1/min)
Deferiprone	0.01	0.05	0.30	0.01
CP363	0.02	0.15	0.16	0.01
CP502	0.00	0.03	0.33	0.00
ICL670	0.01	0.23	0.28	0.00

ICL670. No significant difference was detected between DFO and FeDFO.

DISCUSSION

The Caco-2 cell model has become an important tool in the *in vitro* assessment and prediction of oral permeability in humans. Whereas this cell model has been widely used as an early screening tool for the prediction of *in vivo* intestinal drug absorption for a variety of molecules, and has also been used in studies of iron absorption (17–19), it has not been widely utilized as a model system for iron chelator development. Thus far, despite reports of numerous molecules being synthesized and tested in animal models, only three studies have tested iron-chelating agents in Caco-2 cells (20–22). The present report is, we believe, the first comprehensive bidirectional transport study of iron chelators from three classes of molecular structures, including hexadentate, tridentate, and bidentate compounds, and their iron chelates in Caco-2 monolayers. In addition to determining the mass transport of molecules across Caco-2 monolayers, we have also developed a kinetic model to describe the dynamic movement of chelators from the identifiable cellular compartments.

The apparent permeability coefficients for iron chelators, from both the A-to-B and the B-to-A directions, ranked in decreasing order were as follows: CP363 > deferiprone > ICL670 > CP502 > DFO. With the exception of ICL670, a good agreement is obtained with log $D_{7.4}$. For CP compounds, the higher the lipophilicity, the faster the compound seems to be transported across the monolayers. DFO is not able to cross Caco-2 monolayers, consistent with the understanding that DFO is not absorbed and cannot be given orally because of its high molecular weight (>500) and low lipophilicity (log $D_{7.4} < -0.5$). Although ICL670 is the most lipophilic chelator in our study, it is less permeable compared to CP363 and deferiprone. Because DMSO was needed to dissolve ICL670, we also tested the effect of DMSO on the integrity of the monolayers and the permeability of another chelator (CP363). DMSO at 1% has no effect on the TEER values of the monolayers during the 2-h incubation period. It also did not alter the permeability of CP363 (data not shown). In addition to the lipophilicity, membrane permeability may also be influenced by the ionic state of the compound, with the uncharged molecules generally penetrating cell membranes more readily than charged molecules (23). ICL670 is charged at pH 7.4 because of its benzoate group, whereas CP363 and deferiprone are uncharged at pH 7.4. This may, in part, contribute to observed differences in transport of ICL670, CP363, and deferiprone in the Caco-2 model. Regardless, our studies have demonstrated that for series of homologous compounds, there is a good agreement between their physicochemical properties and the Caco-2 permeabilities. However, when structural diversity is introduced, such relationships are generally weaker (24,25).

Nonpolar transport of CP502, deferiprone, and ICL670 from both directions suggests that these compounds are passively transported, whereas asymmetric transport of CP363, P_{app} (B-to-A) > P_{app} (A-to-B), suggests that efflux

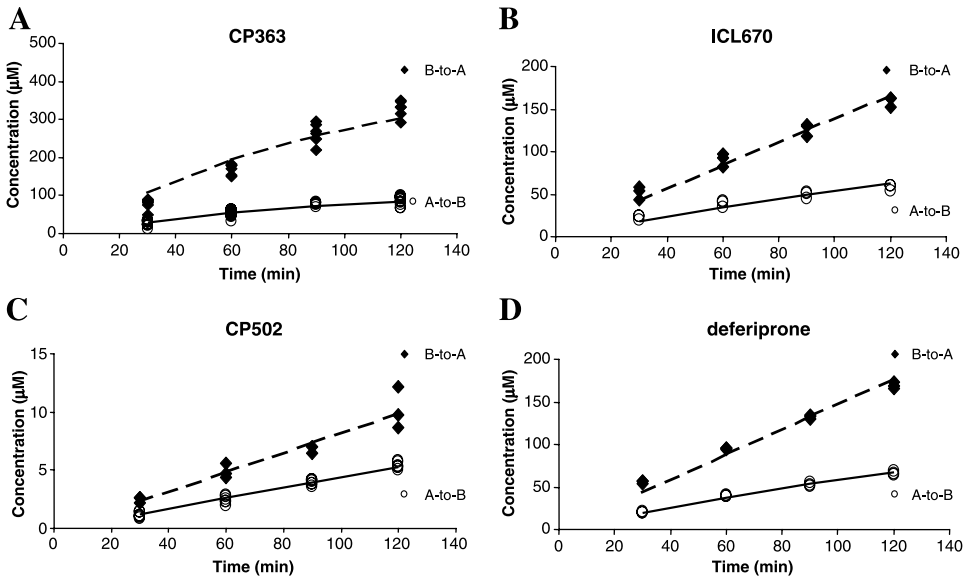

Fig. 8. Computer fitting for bidirectional transport of CP363 (A), ICL670 (B), CP502 (C), and deferiprone (D) under experimental sink conditions. A-to-B: transport from the apical to the basolateral direction; B-to-A: from the basolateral to the apical side. The dashed and solid lines represent the lines of best fit generated by the computer-fitting process.

mechanisms may play a role in the transport of CP363. To test this possibility, a concentration dependence study was performed. A linear relationship between A-to-B and B-to-A transport of CP363 was obtained. However, because of the limitation of the analytical method, we were not able to test concentrations lower than 50 μM. Nonetheless, this result suggests that passive diffusion is primarily responsible for CP363 transport across Caco-2 monolayers; if any active efflux mechanism is involved, its capacity must already be taxed under the tested concentrations.

We also examined the potential influence of P-glycoprotein (Pgp) on transport of CP363. The effect of CP363 on the permeability of Rhodamine-123, a Pgp substrate, was investigated. Our preliminary study showed that CP363 at 500 μM did not increase the P_{app} value of Rhodamine-123 transported from the A-to-B direction, whereas a known Pgp substrate (verapamil at 200 μM) significantly increased the Rhodamine-123 transport (data not shown). Because pH might also play an important role in the transport of weak acid/base compounds, as well as in the permeability of compounds utilizing proton-coupled transporters, it might not have been surprising to observe pH-dependent CP363 transport from A-to-B. However, in our findings, a pH gradient did not alter the transport of CP363 in the A-to-B direction.

Taken together, the Pgp substrate competition and pH-dependent transport studies suggest that CP363 is not a substrate for Pgp, and pH has little effect upon its transport. An explanation or underlying mechanism for the apparent asymmetric transport of CP363 remains to be identified. Further investigations may require a more sensitive analytical methodology, perhaps by using radiolabeled CP363, and further studies that test a broader array of potential transport inhibitors.

Among the iron chelates, $Fe(CP502)_3$, $Fe(ICL670)_2$, and FeDFO were not able to cross Caco-2 monolayers from either direction. In contrast, $Fe(CP363)_3$ and $Fe(deferiprone)_3$ were detectable in the receiving chamber in both directions. However, the amount transported over a 2-h period is less than 0.5% of the applied dose ($P_{app} < 10^{-7}$ cm/s). Because of the limitations of HPLC method, which contained the chelator in the mobile phase, we were not able to identify the nature of the iron transported across the monolayer, namely, as Fe^{3+} or as its 1:3 chelate complex.

The transport of chelates has no correlation with their lipophilicities, which, ranked in decreasing order, were $Fe(CP363)_3 > FeDFO > Fe(ICL670)_2 > Fe(CP502)_3 = Fe(deferiprone)_3$. Transport of $Fe(deferiprone)_3$ across Caco-2 monolayers was also reported previously by Hamilton *et al.* (20). In their study using ^{59}Fe as a tracer, a P_{app} value as high as 2.3×10^{-6} cm/s was reported. This value is about ten times higher than the value from our findings. However, both studies have a very similar P_{app} value for deferiprone transport across the monolayers (2.2×10^{-5} *vs.* 1.3×10^{-5} cm/s, ours *vs.* theirs, respectively).

Other than DFO, the chelators in the study can cross Caco-2 monolayers from both directions, but once they form iron complexes, the permeability of the chelate is altered. The fact that iron chelates, $Fe(CP502)_3$, $Fe(ICL670)_2$, and Fe(DFO), did not pass through Caco-2 monolayers suggests that these iron chelates, if present in the intestine, will not be absorbed.

Prediction of Intestinal Permeability *in Vivo*

Caco-2 monolayers have been demonstrated to be an excellent model to study transport of rapidly and completely absorbed drugs and to predict absorption of this class of drugs in the human intestine (24). It has been demonstrated that compounds that have P_{app} values above 1×10^{-5} cm/s are completely absorbed (>70%) after oral administration in humans; for moderately absorbed compounds (20–70%), the P_{app} values are between 1×10^{-6} and 1×10^{-5} cm/s, and for poorly absorbed compounds (<20%), P_{app} values are less than 1×10^{-6} cm/s. Using this as a guideline, deferiprone, CP363, and ICL670 would be predicted to exhibit high bioavailability after oral administration, CP502 to be incompletely absorbed, and DFO should not be absorbed. Also, their chelates $Fe(CP363)_3$ and $Fe(deferiprone)_3$ would be poorly absorbed (<20%), whereas FeDFO, $Fe(CP502)_3$, and $Fe(ICL670)_2$ should not be absorbed at all. These predictions have been supported through a combination of clinical and preclinical studies for deferiprone, ICL670, and the animal studies of CP363 showing a high bioavailability (26). Because of the low aqueous solubility of ICL670, DMSO was needed to promote solubility, and thus, the comparative permeability with the more soluble hydroxypyridinone chelators may not be clinically relevant because ICL670 might normally be less soluble in the GI fluids. As predicted, DFO is clinically relegated to administration via infusion because of its low bioavailability. However, the prediction for CP502 absorption seems to underestimate its oral bioavailability, as a rat study conducted in our laboratory showed >80% bioavailability of CP502 (27). The limited membrane permeation of CP502 on Caco-2 cells is likely owing to its low lipophilicity.

A potential correlation between *in vitro* transport studies and *in vivo* absorption of the iron chelates remains to be tested. Because of the instability of the chelates under acidic (gastric) conditions, studies to identify the bioavailability of chelates could be problematic. However, *in situ* intestinal perfusion studies might offer an alternative to evaluate chelate absorption. Together with the advantage of the cell culture system to evaluate the permeability of iron chelates, the Caco-2 model should nevertheless serve as an early screening system for oral iron chelator development.

ACKNOWLEDGMENTS

We thank Dr. D. Templeton (University of Toronto) for his review of this manuscript, Dr. R. C. Hider for his advice and the supply of CP363 and FeDFO, Angelo Tesoro and Dr. Jasmina Novakovic for their assistance on HPLC analysis, and Apotex Inc., Canada, for the supply of deferiprone, CP502, ICL670, $Fe(deferiprone)_3$, $Fe(CP363)_3$, and $Fe(CP502)_3$.

REFERENCES

1. M. J. Pippard, S. T. Callender, and D. J. Weatherall. Intensive iron-chelation therapy with desferrioxamine in iron-loading anaemias. *Clin. Sci. Mol. Med.* **54**:99–106 (1978).
2. M. B. Agarwal, C. Viswanathan, J. Ramanathan, D. E. Massil,

S. Shah, S. S. Gupte, D. Vasandani, and R. R. Puniyani. Oral iron chelation with L1. *Lancet* **335**:601 (1990).
3. M. Franchini and and D. Veneri. Iron-chelation therapy: an update. *Hematol. J.* **5**:287–292 (2004).
4. A. Ceci, P. Baiardi, M. Felisi, M. D. Cappellini, V. Carnelli, V. De Sanctis, R. Galanello, A. Maggio, G. Masera, A. Piga, F. Schettini, I. Stefano, and F. Tricta. The safety and effectiveness of deferiprone in a large-scale, 3-year study in Italian patients. *Br. J. Haematol.* **118**:330–336 (2002).
5. O. Han and M. Wessling-Resnick. Copper repletion enhances apical iron uptake and transepithelial iron transport by Caco-2 cells. *Am. J. Physiol.: Gastrointest. Liver Physiol.* **282**:G527–G533 (2002).
6. M. T. Nunez, X. Alvarez, M. Smith, V. Tapia, and J. Glass. Role of redox systems on Fe3+ uptake by transformed human intestinal epithelial (Caco-2) cells. *Am. J. Physiol.* **267**:C1582–C1588 (1994).
7. S. Tandy, M. Williams, A. Leggett, M. Lopez-Jimenez, M. Dedes, B. Ramesh, S. K. Srai, and P. Sharp. Nramp2 expression is associated with pH-dependent iron uptake across the apical membrane of human intestinal Caco-2 cells. *J. Biol. Chem.* **275**:1023–1029 (2000).
8. J. Tennant, M. Stansfield, S. Yamaji, S. K. Srai, and P. Sharp. Effects of copper on the expression of metal transporters in human intestinal Caco-2 cells. *FEBS Lett.* **527**:239–244 (2002).
9. S. Yamaji, J. Tennant, S. Tandy, M. Williams, S. K. Singh Srai, and P. Sharp. Zinc regulates the function and expression of the iron transporters DMT1 and IREG1 in human intestinal Caco-2 cells. *FEBS Lett.* **507**:137–141 (2001).
10. B. Zodl, M. Sargazi, M. Zeiner, N. B. Roberts, I. Steffan, W. Marktl, and C. Ekmekcioglu. Toxicological effects of iron on intestinal cells. *Cell Biochem. Funct.* **22**:143–147 (2004).
11. T. F. Tam, R. Leung-Toung, W. Li, Y. Wang, K. Karimian, and M. Spino. Iron chelator research: past, present, and future. *Curr. Med. Chem.* **10**:983–995 (2003).
12. H. Nick, P. Acklin, R. Lattmann, P. Buehlmayer, S. Hauffe, J. Schupp, and D. Alberti. Development of tridentate iron chelators: from desferrithiocin to ICL670. *Curr. Med. Chem.* **10**:1065–1076 (2003).
13. M. Streater, P. D. Taylor, R. C. Hider, and J. Porter. Novel 3-hydroxy-2(1*H*)-pyridinones. Synthesis, iron(III)-chelating properties, and biological activity. *J. Med. Chem.* **33**:1749–1755 (1990).
14. S. Neuhoff, A. L. Ungell, I. Zamora, and P. Artursson. pH-dependent bidirectional transport of weakly basic drugs across Caco-2 monolayers: implications for drug–drug interactions. *Pharm. Res.* **20**:1141–1148 (2003).
15. Y. Kwon. *Handbook of Essential Pharmacokinetics, Pharmacodynamics, and Drug Metabolism for Industrial Scientists*, Kluwer Academic/Plenum Publishers, New York, 2001.
16. C. A. Lipinski, F. Lombardo, B. W. Dominy, and P. J. Feeney. Experimental and computational approaches to estimate solubility and permeability in drug discovery and development settings. *Adv. Drug Deliv. Rev.* **46**:3–26 (2001).
17. M. N. Garcia, C. Flowers, and J. D. Cook. The Caco-2 cell culture system can be used as a model to study food iron availability. *J. Nutr.* **126**:251–258 (1996).
18. C. Halleux and Y. J. Schneider. Iron absorption by intestinal epithelial cells: 1. CaCo2 cells cultivated in serum-free medium, on polyethyleneterephthalate microporous membranes, as an *in vitro* model. *In Vitro Cell. Dev. Biol.* **27A**:293–302 (1991).
19. C. Halleux and Y. J. Schneider. Iron absorption by CaCo 2 cells cultivated in serum-free medium as *in vitro* model of the human intestinal epithelial barrier. *J. Cell. Physiol.* **158**:17–28 (1994).
20. K. O. Hamilton, L. Stallibrass, I. Hassan, Y. Jin, C. Halleux, and M. Mackay. The transport of two iron chelators, desferrioxamine B and L1, across Caco-2 monolayers. *Br. J. Haematol.* **86**:851–857 (1994).
21. N. Lowther, B. Tomlinson, R. Fox, B. Faller, T. Sergejew, and H. Donnelly. Caco-2 cell permeability of a new (hydroxybenzyl) ethylenediamine oral iron chelator: correlation with physicochemical properties and oral activity. *J. Pharm. Sci.* **87**:1041–1045 (1998).
22. N. Lowther, R. Fox, B. Faller, H. Nick, Y. Jin, T. Sergejew, Y. Hirschberg, R. Oberle, and H. Donnelly. *In vitro* and *in situ* permeability of a 'second generation' hydroxypyridinone oral iron chelator: correlation with physico-chemical properties and oral activity. *Pharm. Res.* **16**:434–440 (1999).
23. A. T. Florence and D. Attwood. *Physicochemical Principles of Pharmacy*, Macmillan, London, 1988.
24. P. Artursson and J. Karlsson. Correlation between oral drug absorption in humans and apparent drug permeability coefficients in human intestinal epithelial (Caco-2) cells. *Biochem. Biophys. Res. Commun.* **175**:880–885 (1991).
25. D. Sun, H. Lennernas, L. S. Welage, J. L. Barnett, C. P. Landowski, D. Foster, D. Fleisher, K. D. Lee, and G. L. Amidon. Comparison of human duodenum and Caco-2 gene expression profiles for 12,000 gene sequences tags and correlation with permeability of 26 drugs. *Pharm. Res.* **19**:1400–1416 (2002).
26. F. Guo, J. J. Thiessen, A. Tesoro, and M. Spino. High-performance liquid chromatographic assays for a second-generation novel oral iron chelator (APCP363) and their application to pharmacokinetic studies in rats. *J. Chromatogr., B, Biomed. Sci. Appl.* **751**:107–115 (2001).
27. J. Novakovic, A. Tesoro, M. Spino, and J. Thiessen. Improved high-performance liquid chromatographic method for the pharmacokinetic studies of a novel iron chelator, CP502, in rats. *J. Chromatogr., B, Analyt. Technol. Biomed. Life Sci.* **796**:105–112 (2003).
28. E. Liang, K. Chessic, and M. Yazadanian. Evaluation of an accelerated Caco-2 cell permeability model. *J. Pharm. Sci.* **89**:336–345 (2000).